Mycobiology

Research Article

Role of MAPK Signaling Pathways in Regulating the Hydrophobin Cryparin in the Chestnut Blight Fungus *Cryphonectria parasitica*

Kum-Kang So and Dae-Hyuk Kim*

Department of Molecular Biology, Department of Bioactive Material Sciences, Institute for Molecular Biology and Genetics, Chonbuk National University, Jeonju 54896, Korea

Abstract We assessed the regulation of cryparin, a class II hydrophobin, using three representative mitogen-activated protein kinase (MAPK) pathways in *Cryphonectria parasitica*. Mutation of the *CpSlt2* gene, an ortholog of yeast *SLT2* in the cell wall integrity (CWI) pathway, resulted in a dramatic decrease in cryparin production. Similarly, a mutant of the *CpBck1* gene, a MAP kinase kinase kinase gene in the CWI pathway, showed decreased cryparin production. Additionally, mutation of the *cpmk*1 gene, an ortholog of yeast *HOG1*, showed decreased cryparin production. However, mutation of the *cpmk*2 gene, an ortholog of yeast Kss1/Fus3, showed increased cryparin production. The easy-wet phenotype and accumulation of the cryparin transcript in corresponding mutants were consistent with the cryparin production results. *In silico* analysis of the promoter region of the cryparin gene revealed the presence of binding motifs related to downstream transcription factors of CWI, HOG1, and pheromone responsive pathways including MADS-box- and Ste12-binding domains. Real-time reverse transcriptase PCR analyses indicated that both *CpRlm1*, an ortholog of yeast *RLM1* in the CWI pathway, and *cpst12*, an ortholog of yeast *STE12* in the mating pathway, showed significantly reduced transcription levels in the mutant strains showing lower cryparin production in *C. prasitica*. However, the transcription of *CpMcm1*, an ortholog of yeast *MCM1*, did not correlate with that of the mutant strains showing downregulation of cryparin. These results indicate that three representative MAPK pathways played a role in regulating cryparin production. However, regulation varied depending on the MAPK pathways: the CWI and HOG1 pathways were stimulatory, whereas the pheromone-responsive MAPK was repressive.

Keywords Cryparin, *Cryphonectria parasitica*, Hydrophobin, MADS-box transcription factor, Mitogen-activated protein kinase signaling pathway

Fungal hydrophobins are small, secreted proteins that react to the outermost interface of an object, typically conferring a hydrophobic property on fungal cell walls [1, 2]. These proteins have been found to impact several morphogenetic processes, including sporulation, fruit body development, and infection structure formation [2]. Cryparin (*Crp*) is a small, abundant cell-surface hydrophobic protein in chestnut blight fungus *Cryphonectria parasitica*; it is a class II hydrophobin [1, 3, 4]. Antibody staining has indicated that cryparin is exclusively abundant in the fungal fruiting body walls on its natural host, although it has also been found on the surfaces of fungal hyphae grown in artificial culture. Functional analysis of cryparin has indicated that it is required for stromal pustule eruption through the bark of the chestnut tree; this function plays an essential role in the fitness of the fungus [4]. In *C. parasitica*, *Crp* mRNA is abundantly expressed, and the cryparin transcript has been shown to account for 25–30% of the total mRNA after 2 days of liquid culture [5]. Promoter analysis of the cryparin gene has indicated that it contains a small core promoter region, which is necessary for high cryparin expression levels [6]. Interestingly, the infection of *C. parasitica* by Cryphonectria hypovirus 1 (CHV1) results in a drastic change in the accumulation of *Crp* mRNA, and *Crp* expression has been shown to be transcriptionally downregulated (between 50% and 70%) in a CHV1-713-infected strain (UEP1), compared with an isogenic virus-free strain (EP155/2) [4, 5]. However, no other regulatory mechanisms have been characterized for cryparin regulation.

Mycobiology 2017 December, **45**(4): 362-369
https://doi.org/10.5941/MYCO.2017.45.4.362
pISSN 1229-8093 • eISSN 2092-9323

***Corresponding author**
E-mail: dhkim@jbnu.ac.kr

Received October 1, 2017
Revised October 6, 2017
Accepted October 15, 2017

Signaling cascades play critical roles in modulating diverse regulators, including protein kinases and transcription factors. Among these, the mitogen-activated protein kinase (MAPK) signaling pathway is of particular interest because several genes in the MAPK pathways of *C. parasitica* and their downstream effectors are closely implicated in symptom development such as reduced sporulation, pigmentation, laccase production, and virulence by the hypovirus infection [7-14]. The MAPK signal transduction pathway consists of three functionally interlinked cascade kinases: MAP kinase kinase kinase, MAP kinase kinase, and MAP kinase (MAPK). The MAPK pathways are highly conserved across a wide range of organisms from yeast to humans [15, 16]. In the most studied fungus *Saccharomyces cerevisiae*, five different MAPK pathways, governing pheromone response, filamentous growth, osmotolerance (HOG1), cell wall integrity (CWI), and ascospore formation, have been identified [17]. As an analogy, three signaling pathways regulating the pheromone response, CWI, and the osmoregulation/stress response have been suggested in filamentous fungi [18]. Fungal hydrophobins, in general, play an important role in the growth and development of most fungi [19]. Thus, both biotic and abiotic environmental conditions have been proven to affect the expression of hydrophobin genes and various signaling pathways such as cAMP/PKA, Ca^{2+}/calmodulin, MAPK, and the cell cycle have been identified as regulatory pathways for fungal hydrophobin expression [20-24]. Among these, MAPK signaling pathways are particularly promising. Depending on the fungi, different MAPK pathways have been implicated in the regulation of hydrophobin. Specifically, PMK1, an ortholog of yeast Kss1/Fus3, was shown to regulate the MPG1 hydrophobin gene in *Magnaporthe oryzae*, and *VdHog1*, an ortholog of yeast *HOG1*, was shown to be essential in the expression of VDH1 hydrophobin in *Verticillium dahliae* [22, 25].

In this study, using the advantage of the availability of mutants in three representative MAPKs, we explored the MAPK regulation of cryparin production in *C. parasitica*.

MATERIALS AND METHODS

Fungal strains and culture conditions. *C. parasitica* strains used in this study are listed in Table 1. Strains were grown on potato dextrose agar containing L-methiononine (100 mg/L) and biotin (1 mg/L) (PDAmb) plates under constant low light at 25°C [26]. The mycelia were harvested from 5-day-old cultures, lyophilized, and stored at −70°C for RNA extraction as previously described [27].

Hydrophobicity of mycelial mats. Hydrophobicity of the mycelia of 7-day-old cultures was evaluated by observing the assimilation of 9–10 water droplets (3 μL each) on mycelial surfaces on culture plates.

Cryparin extraction from mycelia. Lyophilized mycelia of 7-day-old cultures were finely ground, well suspended in 60% ethanol (5 μL ethanol per 1 mg mycelia) and centrifuged at 8,000 ×g for 15 min [3]. Extracts from all preparations were further suspended in 6× polyacrylamide gel electrophoresis (PAGE) loading dye and 15% glycerol, followed by separation on a 12% sodium dodecyl sulfate (SDS)-PAGE gel. Following separation, gels were stained with Coomassie blue to visualize the extracted proteins.

Cloning and characterization of MADS-box transcription factors. The *C. parasitica* genome database (http://genome.jgi-psf.org/Crypa1/Crypa1.home.html) was screened for yeast MCM1 and RLM1 homologues. Polymerase chain reaction (PCR) amplification of *CpMcm1* and *CpRlm1* was performed with primers CpMcm1-gF1/CpMcm1-gR1 and CpRlm1-gF1/CpRlm1-gR1, respectively (Table 2). The resulting 1.6-kb PCR amplicon of *CpMcm1* and 5.1-kb amplicon of *CpRlm1* were cloned separately into the pGEM-T Easy vector (Promega, Madison, WI, USA) and sequenced.

To obtain cDNA clones of *CpMcm1* and *CpRlm1*, PCR was performed using reverse transcriptase PCR (RT-PCR) with primers CpMcm1-mF1/CpMcm1-mR1 and CpRlm1-mF1/CpRlm1-mR1 at nucleotide positions (nt) −1 to 19/917 to 937 and (nt) −15 to 7/1,961 to 1,981 (relative to the start codon). The resulting 0.7-kb PCR amplicon of *CpMcm1* and 1.8-kb amplicon of *CpRlm1* were cloned separately into the pGEM-T Easy vector and sequenced.

Phylogenetic analysis of MADS-box transcription factors. The phylogenetic relationships of *CpMcm1* and *CpRlm1* with other fungal MADS-box transcription factor

Table 1. List of strains in this study

Strain	Chracter	Reference
EP155/2	Wild-type of *Cryphonectria parasitica*	ATCC 38755
UEP1	CHV1-infected strain, isogenic strain of EP155/2	ATCC 38751
Δ*Crp*	*Crp*-null mutant	[4]
TdBCK1	*CpBck1*-null mutant	[13]
TdBCK1-S1	Sectored progeny of TdBCK1	[13]
TdSLT2-69	*CpSlt2*-null mutant	[14]
TdSLT2-69-S1	Sectored progeny of TdSLT2-69	[14]
TdMK1-23	*cpmk*1-null mutant	[8]
TdMK2-1	*cpmk*2-null mutant	[10]

Table 2. List of primer sequences

Primer	Sequence (5′ to 3′)	Method
CpMcm1-gF1	TGCCGCTTGTGTCACTTTGT	PCR[a]
CpMcm1-gR1	GGCAATTAGGCTGCACCAGT	PCR
CpRlm1-gF1	TGGACGTTGTACCATCGCAGG	PCR
CpRlm1-gR1	TCCAGGATGTGAGGACCAAACCT	PCR
CpMcm1-mF1	CATGGCCGACATCACAGACC	RT-PCR
CpMcm1-mR1	TCTTATGACTGGTGTTGGGCA	RT-PCR
CpRlm1-mF1	GTCGACGACTTCATCATGGGTC	RT-PCR
CpRlm1-mR1	GTCTTTCACTAGTTTTCAACC	RT-PCR
Gpd_RT_F1	CCGTCAACGACCCCTTCAT	qRT-PCR
Gpd_RT_R1	GTTGCCGTGTTGAGAGTCATACTT	qRT-PCR
cryparin_RT_F1	CTCCACGACCTACACCGCTT	qRT-PCR
cryparin_RT_R1	AGTCTCGCAGTCCAGGTCAG	qRT-PCR
cpst12_RT_F1	GCATTCTCCAGATCAGACAACCT	qRT-PCR
cpst12_RT_R1	AGGTTCAGTCCATCGACTCCAT	qRT-PCR
CpMcm1_RT_F1	GTCGCCACATCACCTTCTCG	qRT-PCR
CpMcm1_RT_R1	TCCGAGACGACGAGCAGTAG	qRT-PCR
CpRlm1_RT_F1	ATGCTGAACACTACGTCCGC	qRT-PCR
CpRlm1_RT_R1	CTGCCAGATGTTGCGACAGT	qRT-PCR

RT-PCR, reverse transcriptase PCR; qRT-PCR, quantitative real-time PCR.
[a]PCR to obtain full gene.

homologs were analyzed using MEGA 7 [28]. An evolutionary matrix was inferred using the Henikoff and Henikoff (1992) method [29], and the branching pattern was generated using the neighbor-joining method [30, 31].

Analysis of transcript accumulation using quantitative real-time RT-PCR. RNA from all tested strains was extracted from culture 5 days after inoculation, and quantitative real-time RT-PCR was conducted as previously described [10]. Analyses were conducted at least twice, in triplicate for each transcript, from at least two independent RNA preparations of the same sample. Transcript levels relative to the amount of glyceraldehyde-3-phosphate dehydrogenase (*gpd*) of *C. parasitica* were used as an internal control. The primer pairs used for each target gene are listed in Table 2.

Statistical analyses. All quantitative real-time RT-PCR transcripts were analyzed by ANOVA using SPSS software ver. 23.0 (IBM Corp., Armonk, NY, USA). The significance of all effects was determined using the Student-Newman-Keuls method at $p = 0.001$.

RESULTS AND DISCUSSION

Phenotypic changes of MAPK mutants. To determine the surface hydrophobicity of the aerial mycelia, the easy-wet phenotype was screened by placing a water droplet on the surface of aerial hyphae that had grown for 7 days on PDAmb. Normally, when applying a water droplet to the surface of aerial hyphae, the surface hydrophobicity of the hyphae prevents the water droplet from being absorbed by aerial mycelia and the water remains a discrete drop.

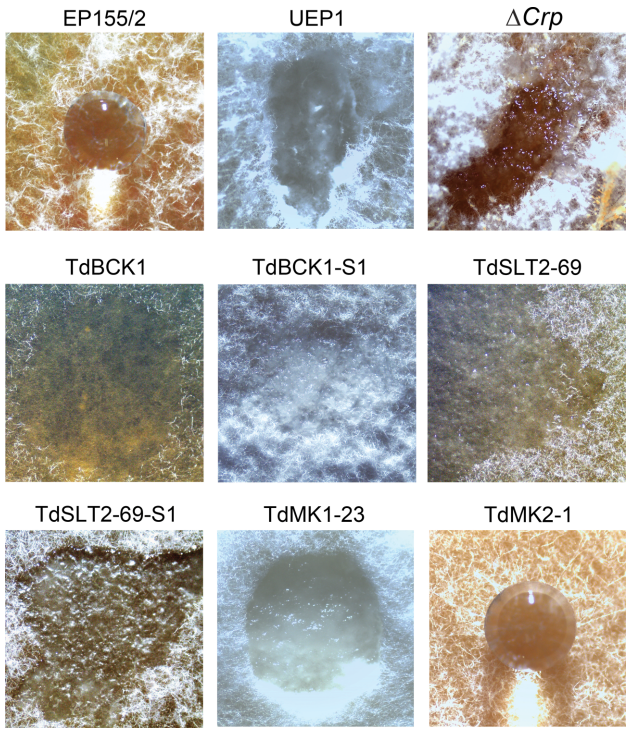

Fig. 1. Easy-wet morphology to determine the hydrophobicity of mycelia. Wild-type EP155/2, hypovirulent UEP1, cryparin-null mutant (Δ*Crp*), *CpBck1*-null mutant (TdBCK1), a sectored progeny of TdBCK1 (TdBCK1-S1), *CpSlt2*-null mutant (TdSLT2-69), a sectored progeny of TdSLT2-69 (TdSLT2-69-S1), *cpmk*1-null mutant (TdMK1-23), and *cpmk*2-null mutant (TdMK2-1) strains are indicated on the panels. Colonies are shown after 7 days of culture. After dropping 3 μL of water on the mycelial surfaces, easy-wet morphology was observed using microscopy (EZ4HD, Leica, Germany).

However, a cryparin-null mutant quickly absorbs the drop of water. Therefore, we examined the easy-wet phenotype of the mutants representing the three MAPK pathways (Fig. 1). The wild-type EP155/2 showed non-absorbed, intact water droplets and the water drops remained intact even after long periods of incubation (> 24 hr). However, the cryparin-null mutant quickly adsorbed the water droplet, a response characteristic of the easy-wet phenotype [4]. Both the *CpSlt2*-null mutant and its sectored progeny exhibited the absorption of water droplets, indicating changes in the surface hydrophobicity of the aerial mycelia. The hydrophobicity of the *CpBck1*-null mutant was also estimated using water droplets. However, the near absence of aerial hyphae in the *CpBck1*-null mutant made it difficult to determine the surface hydrophobicity. Thus, the easy-wet phenotype was measurable only in the sectored progeny of the *CpBck1*-null mutant. The sectored progeny of the *CpBck1*-null mutant exhibited the characteristic easy-wet phenotype, although compact aerial mycelia were produced on the colony of the sectored progeny, and not on the parental *CpBck1*-null mutant. These results clearly indicate that mutants in the CWI pathways have impaired surface hydrophobicity. We also tested the surface hydrophobicity of the mutant in the mating-responsive MAPK pathway. The mutation in the *cpmk*2 gene, an ortholog of yeast *FUS3* gene, resulted in different growth patterns in response to solid and liquid media [11]. The *cpmk*2-null mutant showed reduced colonial growth but no growth defect in liquid media. Interestingly, absorption of water droplets on top of the aerial mycelia was not observed (> 24 hr), indicating that the surface hydrophobicity was not changed. Previous studies on the *cpmk*1 mutant, an ortholog of the yeast *HOG1* gene, demonstrated that transcription of the cryparin gene was severely downregulated, such that it was even lower than that of the hypovirulent UEP1 strain, which has been known to downregulate the cryparin gene. It has been reported that the easy-wet phenotype on the aerial mycelia is not obvious [10]. We verified the easy-wet phenotypes of the *cpmk*1-null mutant and the hypovirulent UEP1 strain and found that in both most water droplets were completely absorbed after long periods of incubation. This difference between the current study and previous studies may be attributed to different colony ages, adaptive changes of the mutants during long periods of storage, or uneven distribution of surface hydrophobicity.

To gain a better understanding of the amount of cryparin produced, we extracted cryparin from the mycelia of mutants and compared cryparin amounts using SDS-PAGE. As shown in Fig. 2A, a protein band was observed at 24 kDa for cryparin in wild-type EP155/2. It is well known that, compared with wild-type EP155/2, cryparin is significantly downregulated in the CHV1-infected isogenic strain UEP1, which was represented by a very-intensity cryparin band on SDS-PAGE (Fig. 2A). In *CpBck1*-, *CpSlt2*-, and *cpmk*1-null mutants exhibiting the easy-wet phenotype, the cryparin band was nearly absent. Interestingly, a more than two-fold

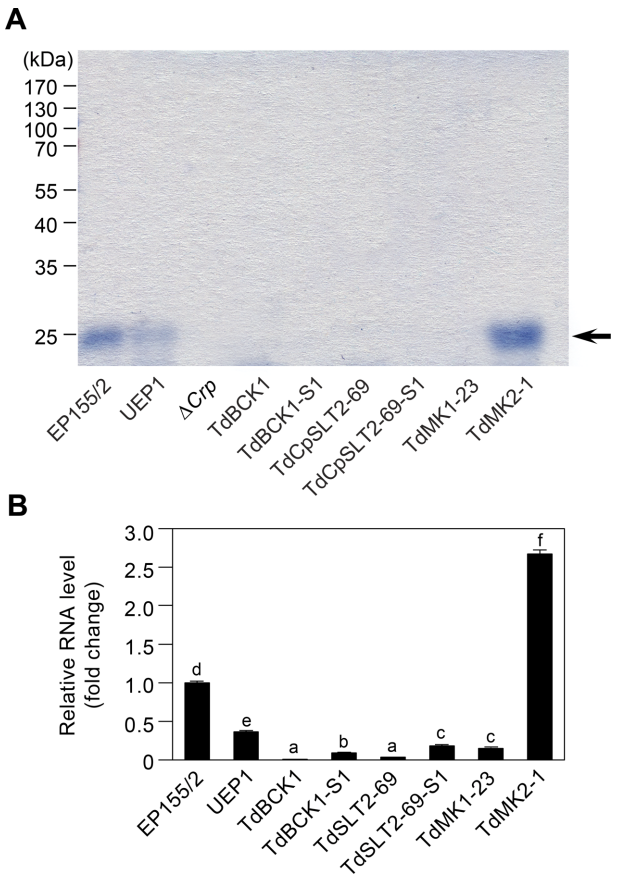

Fig. 2. The cryparin production (A) and cryparin transcript (B) of mitogen-activated protein kinase pathway mutants. Wild-type EP155/2, hypovirulent UEP1, *Crp*-null mutant (Δ*Crp*), *CpBck1*-null mutant (TdBCK1), a sectored progeny of TdBCK1 (TdBCK1-S1), *CpSlt2*-null mutant (TdSLT2-69), a sectored progeny of TdSLT2-69 (TdSLT2-69-S1), *cpmk*1-null mutant (TdMK1-23), and *cpmk*2-null mutant (TdMK2-1) strains are shown.

increase of cryparin band intensity was observed in the *cpmk*2-null mutant, suggesting that more cryparin was produced in the *cpmk*2-null mutant. We also examined the accumulation of cryparin transcript among mutants using real-time RT-PCR (Fig. 2B). The accumulation of cryparin transcripts was significantly downregulated in strains exhibiting the easy-wet phenotype and less amount of cryparin. Cryparin transcript was significantly increased in the *cpmk*2-null mutant, indicating increased cryparin production. Analyses of cryparin expression indicated that only two MAPK pathway-related mutants, CWI and Hog1, exhibited clear easy-wet phenotypes, due to the dramatic decrease in cryparin production. The Fus3 MAPK pathway mutant also appeared to be implicated in cryparin production, but in a different way from the other two MAPK pathways. The results regarding on the easy-wet phenotype, protein production, and transcript accumulation were all consistent with one another, and the modulation of cryparin production occurred at the level of transcription, according to real-

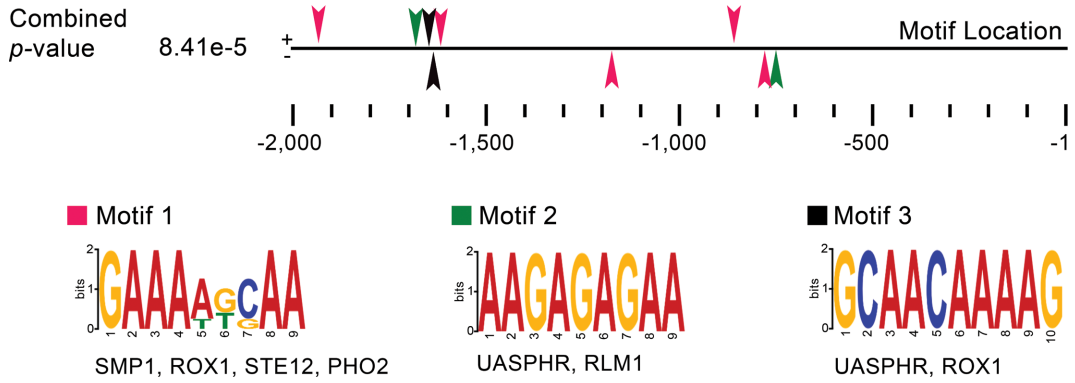

Fig. 3. Regulatory motifs of the cryparin promoter in *Cryphonectria parasitica*. Predictions were obtained from MEME-suite and TOMTOM analysis. Pink, green, and black wedge-shapes indicate motifs 1, 2, and 3, respectively.

time RT-PCR.

***In silico* analysis of regulatory motifs in the cryparin gene promoter.** Regulatory sequence motifs were sought and discovered in the 2.0 kb-promoter region of the cryparin gene, which includes the core 188-bp promoter region, using the MEME suites [32]. MEME analysis demonstrated that the promoter region contained three types of binding motifs at a combined *p*-value of 8.41e-5 (Fig. 3). Motif 1 occurred five times and motifs 2 and 3 each occurred twice in the promoter region (Fig. 3). Using the yeast motif database SCPD, the motif database-scanning algorithm TOMTOM identified regulatory elements corresponding to binding motifs [33]. The regulatory elements corresponding to motif 1 were stress responsive myocyte enhancer factor 2 (MEF2)-like transcription factor regulated by Hog1 (SMP1), high mobility group box containing transcriptional repressor for lowering sterol content in response to high osmolarity Hog1 and hypoxic repressor (ROX1), homeodomain divergent, pheromone-responsive transcriptional activator (STE12), and homeodomain transcriptional activator of phosphate signal transduction (PHO) pathway (PHO2). The regulatory elements of UASPHR (PHR1 upstream activator sequence sites, a hallmark of genes involved in nucleotide excision repair and recombination, UAS for MGT1, RAD16, RAD9, RAD23, RAD51, MAG1, RAD4, RAD6, RNR3, RNR2, RAD26, RAD7, RAD52, RAD50, PHR1, RAD1, MEC2, SPK1, RAD53, and MGTR) and stress responsive MEF2-like transcription factor regulated by Bck1 (RLM1) were identified as regulatory elements, which likely bind motif 2. UASPHR and ROX1 were identified for motif 3.

Transcription of *in silico*-suggested transcription factors for cryparin expression. Among the diverse regulatory motifs, the SMP1, STE12, RLM1 binding motifs were of interest because SMP1, STE12, and RLM1 are well-known downstream transcriptional regulators of MAPK pathways in response to high osmolarity, pheromone, and CWI, respectively [34, 35]. The SMP1 binding motif is the MADS-box binding motif, which is involved in interactions of the transcription factor containing the MADS-box domain, a conserved amino acid region for DNA binding and dimerization [36]. Based on the sequence similarity, MADS-box proteins are classified as a serum response factor (SRF)-like/Type I and MEF2-like/Type II subfamily. Although *S. cerevisiae* harbors four MADS-box proteins, a survey of the *C. parasitica* genome revealed the presence of two MADS-box transcription factors, *CpRlm1* and *CpMcm1*, which were similar to those of other known filamentous ascomycetes [37]. The genomic and near full-length cDNA of *CpRlm1* and *CpMcm1* were cloned and sequenced using gene-specific primers and RT-PCR as previously described (Table 2) [8-10]. Sequence analysis of *CpRlm1* indicated that it consisted of three exons, with two intervening sequences of 106 and 82 bp. The deduced protein product consisted of 594 amino acids, with an estimated molecular mass of 64.3 kDa and a pI of 9.28 (GenBank accession No. MF969091). *CpMcm1* was predicted to consist of three exons, with two intervening sequences of 202 and 79 bp. The deduced protein product consisted of 217 amino acids, with an estimated molecular mass of 23.5 kDa and a pI of 5.97 (GenBank accession No. MF969092). A homology search of *CpRlm1* using the Clustal Omega software revealed that the protein product showed high amino acid identities with other known MADS-box transcription factors of *Aspergillus nidulans* RlmA (42% amino acid [aa] identity), *A. fumigatus* RlmA (47%), *Neurospora crassa* Rlm1 (52%), *Fusarium graminearum* Rlm1 (57%), *M. oryzae* MIG1 (64%), and *S. cerevisiae* Rlm1 (26%). In addition, a homology search of *CpMcm1* demonstrated high amino acid identities with other known MADS-box transcription factors of *A. nidulans* McmA (63% aa identity), *A. fumigatus* Mcm1 (64%), *F. graminearum* FgMcm1 (74%), *N. crassa* Mcm1 (75%), and *S. cerevisiae* Mcm1 (49%). However, very limited similarity (33.1%) was observed between the protein products of *CpRlm1* and *CpMcm1*. Phylogenetic analysis of *CpRlm1* and *CpMcm1* indicated that *CpMcm1* belonged to the clade containing an SRF-like subfamily, and *CpRlm1* belonged to the clade containing a MEF2-like subfamily (Fig. 4).

The accumulation of *CpRlm1*, *CpMcm1*, and *cpst12*

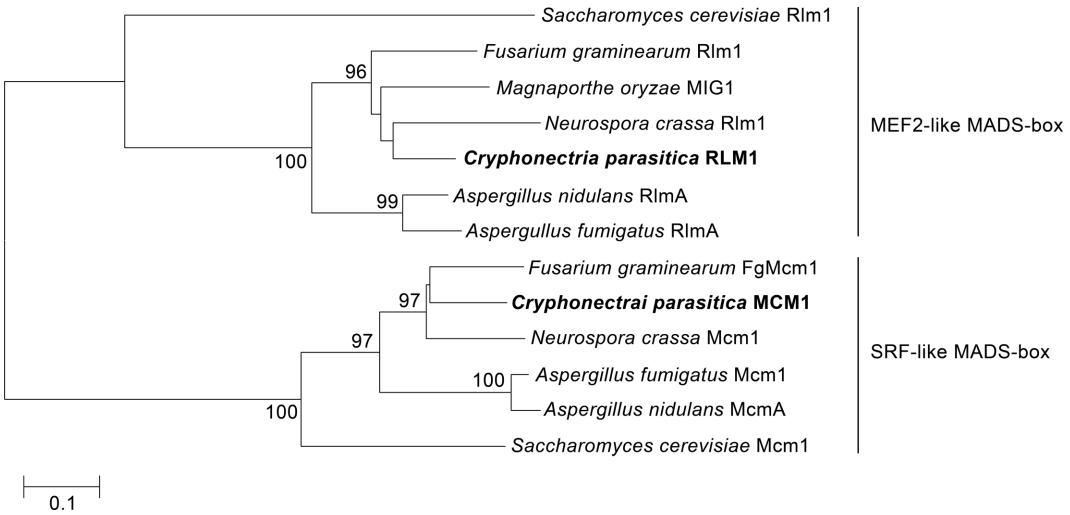

Fig. 4. Phylogenetic analysis of the *CpMcm1* and *CpRlm1* genes of *Cryphonectria parasitica*. Phylogenetic tree was generated using the neighbor-joining method with selected ascomycetes: Mcm1 (CAA88409.1) and Rlm1 (AAB68210.1) from *Saccharomyces cerevisiae*, MIG1 (ABX79379.1) from *Magnaporthe oryzae*, FgMcm1 (XP_388872.1) and Rlm1 (XP_389515.1) from *Fusarium graminearum*, Mcm1 (EAA35381.1) and Rlm1 (EAA36453.3) from *Neurospora crassa*, Mcm1 (EAL85828.1) and RlmA (EAL92725.1) from *Aspergillus fumigatus*, McmA (EAA60098.1) and RlmA (EAA63555.1) from *A. nidulans*. Numbers at the nodes indicate bootstrap values (> 90). Bootstrap analysis was performed with 1,000 replications. Bar represents 10% sequence divergence. MEF2, myocyte enhancer factor 2; SRF, serum response factor.

transcripts was analyzed using real-time RT-PCR. In order to understand the downregulation of cryparin and the easy-wet phenotype, we examined the expression of putative regulatory elements using real-time RT-PCR. The accumulation of *CpRlm1* transcript was significantly reduced in the *CpBck1* and *CpSlt2* mutant strain in the CWI MAPK pathway, suggesting that the cloned *CpRlm1* appeared to be the downstream transcription factor of the CWI pathway (Fig. 5A). Compared with the wild type, transcription of the *CpRlm1* gene was significantly downregulated in *Crp*- and *cpmk*1-null mutant strains, which exhibited the easy-wet phenotype and reduced amounts of cryparin. However, no significant changes in the *CpRlm1* transcript were observed in the hypovirulent UEP1 strain, which showed reduced amounts of cryparin and the corresponding transcript. These results suggest that *CpRlm1* is important for the expression of cryparin, but that the hypoviral regulation of cryparin may not be directly attributed to *CpRlm1*. When we examined the accumulation of *CpMcm1* transcripts, the *CpMcm1* transcript was not significantly changed in UEP1 and the sectored progeny of the *CpBck1*-null mutant, which showed reduced amounts of cryparin and their transcription. More interestingly, the accumulation of the *CpMcm1* transcript was significantly increased in the cryparin-null mutant (Fig. 5B). These results indicate that *CpMcm1* had very little effect on cryparin expression. We also analyzed the transcription of *cpst12*, an ortholog of yeast *STE12* [9, 10]. The accumulation of *cpst12* was significantly reduced in mutant strains of *cpmk*2, an ortholog of yeast *FUS3*, which suggested that the *cpst12* was a downstream transcription factor of *cpmk*2. In tested strains showing the easy-wet phenotype and reduced amounts of cryparin, the accumulation of *cpst12* transcript was significantly decreased compared with that of the wild-type EP155/2 (Fig. 5C). Thus, *cpst12* appeared to be essential for cryparin expression. *cpst12* was transcriptionally downregulated in the *cpmk*2-null mutant showing the increased cryparin production. Considering that *cpst12* is a downstream factor of *cpmk*2, its downregulation in the *cpmk*2 mutant is not uncommon. However, the *cpmk*2-null mutant demonstrated increased cryparin in terms of transcript accumulation and protein levels. Additionally, the accumulation of *CpRlm1* transcript was also downregulated in the *cpmk*2-null mutant. Thus, the modulation of cryparin expression appears to be more complex in that, although transcriptional regulation by both *CpRlm1* and *cpst12* occurred, there might be another tier of regulation mediated by a pheromone-responsive pathway. Thus, it will be interesting to examine cryparin production in the *CpRlm1*- and *cpst12*-null mutant strains.

In conclusion, the promoter region of the class II fungal hydrophobin cryparin contained a MADS-box binding element and *cpst12*-binding domain. Among the two putative MADS-box transcription factors of *C. parasitica*, *CpRlm1*, not *CpMcm1*, was the putative transcription factor that showed dramatic transcriptional downregulation in mutant strains exhibiting the easy-wet phenotype. Additionally, *cpst12* is a putative transcription factor, showing a transcript downregulation pattern in mutant strains with the easy-wet phenotype and reduced amounts of cryparin. Thus, among three characterized MAPK pathways, two pathways, *cpmk*1 and *CpSlt2*, orthologs of yeast *HOG1* and *SLT2*, respectively, showed downregulation of *CpRlm1* and transcriptional

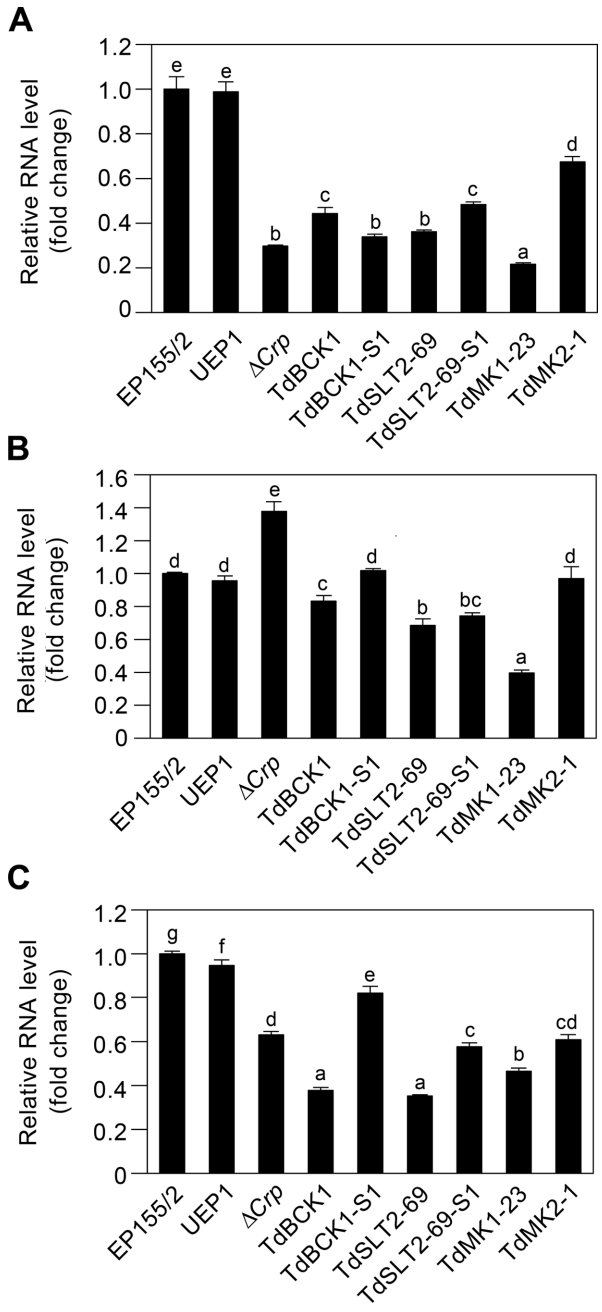

Fig. 5. Quantitative real-time reverse transcription polymerase chain reaction analysis of *cpst12*, *CpMcm1*, and *CpRlm1*. Changes in expression of *CpRlm1* (A), *CpMcm1* (B), and *cpst12* (C) with the wild-type (EP155/2), hypovirulent (UEP1), *Crp*-, *CpBck1*-, *CpSlt2*-, *cpmk*1-, and *cpmk*2-null mutant strains relative to levels of glyceraldehyde-3-phosphate dehydrogenase (*gpd*). Y-axis values were normalized to the transcript levels of the corresponding gene in the wild-type strain. Error bars indicate standard deviation based on three independent measurements.

downregulation of cryparin (Fig. 5). These results suggest that *CpRlm* and *cpst12* might be putative transcription factors for the motif in the promoter region of cryparin. However, further studies on the binding affinity of *CpRlm1* and *cpst12* to the motif in the cryparin promoter region should be conducted to examine specific downstream effects of cryparin expression.

In response to extreme changes in the environment, precise responses must be coordinated by the fungi through MAPK signaling pathways. Our studies provide a framework for examining comparative studies of MAPK signaling and indicate that all three MAPK pathways play a role in the regulation of the fungal hydrophobin cryparin in *C. parasitica*.

ACKNOWLEDGEMENTS

This work was supported by the NRF grants by MSIP (2015R1A2A1A10055684). We thank the Institute of Molecular Biology and Genetics at Chonbuk National University for kindly providing the facilities for this research. K. K. So was supported by BK21 PLUS program in the Department of Bioactive Material Sciences.

REFERENCES

1. Wessels JG. Hydrophobins: proteins that change the nature of the fungal surface. Adv Microb Physiol 1997;38:1-45.
2. Wösten HA. Hydrophobins: multipurpose proteins. Annu Rev Microbiol 2001;55:625-46.
3. Carpenter CE, Mueller RJ, Kazmierczak P, Zhang L, Villalon DK, Van Alfen NK. Effect of a virus on accumulation of a tissue-specific cell-surface protein of the fungus *Cryphonectria (Endothia) parasitica*. Mol Plant Microbe Interact 1992;5:55-61.
4. Kazmierczak P, Kim DH, Turina M, Van Alfen NK. A hydrophobin of the chestnut blight fungus, *Cryphonectria parasitica*, is required for stromal pustule eruption. Eukaryot Cell 2005;4:931-6.
5. Zhang L, Villalon D, Sun Y, Kazmierczak P, Van Alfen NK. Virus-associated down-regulation of the gene encoding cryparin, an abundant cell-surface protein from the chestnut blight fungus, *Cryphonectria parasitica*. Gene 1994;139:59-64.
6. Kwon BR, Kim MJ, Park JA, Chung HJ, Kim JM, Park SM, Yun SH, Yang MS, Kim DH. Assessment of the core cryparin promoter from *Cryphonectria parasitica* for heterologous expression in filamentous fungi. Appl Microbiol Biotechnol 2009;83:339-48.
7. Deng F, Allen TD, Hillman BI, Nuss DL. Comparative analysis of alterations in host phenotype and transcript accumulation following hypovirus and mycoreovirus infections of the chestnut blight *fungus Cryphonectria parasitica*. Eukaryot Cell 2007;6:1286-98.
8. Park SM, Choi ES, Kim MJ, Cha BJ, Yang MS, Kim DH. Characterization of HOG1 homologue, CpMK1, from *Cryphonectria parasitica* and evidence for hypovirus-mediated perturbation of its phosphorylation in response to hypertonic stress. Mol Microbiol 2004;51:1267-77.
9. Park JA, Kim JM, Park SM, Kim DH. Characterization of *CpSte11*, a MAPKKK gene of *Cryphonectria parasitica*, and initial evidence of its involvement in the pheromone response pathway. Mol Plant Pathol 2012;13:240-50.

10. Choi ES, Chung HJ, Kim MJ, Park SM, Cha BJ, Yang MS, Kim DH. Characterization of the ERK homologue CpMK2 from the chestnut blight fungus *Cryphonectria parasitica*. Microbiology 2005;151(Pt 5):1349-58.
11. Sun Q, Choi GH, Nuss DL. Hypovirus-responsive transcription factor gene *pro1* of the chestnut blight fungus *Cryphonectria parasitica* is required for female fertility, asexual spore development, and stable maintenance of hypovirus infection. Eukaryot Cell 2009;8:262-70.
12. Turina M, Zhang L, Van Alfen NK. Effect of *Cryphonectria hypovirus 1* (CHV1) infection on Cpkk1, a mitogen-activated protein kinase kinase of the filamentous fungus *Cryphonectria parasitica*. Fungal Genet Biol 2006;43:764-74.
13. Kim JM, Lee JG, Yun SH, So KK, Ko YH, Kim YH, Park SM, Kim DH. A mutant of the *Bck1* homolog from *Cryphonectria parasitica* resulted in sectorization with an impaired pathogenicity. Mol Plant Microbe Interact 2016;29:268-76.
14. So KK, Ko YH, Chun J, Kim JM, Kim DH. Mutation of the *Slt2* ortholog from *Cryphonectria parasitica* results in abnormal cell wall integrity and sectorization with impaired pathogenicity. Sci Rep 2017;7:9038.
15. Herskowitz I. MAP kinase pathways in yeast: for mating and more. Cell 1995;80:187-97.
16. Schaeffer HJ, Weber MJ. Mitogen-activated protein kinases: specific messages from ubiquitous messengers. Mol Cell Biol 1999;19:2435-44.
17. Gustin MC, Albertyn J, Alexander M, Davenport K. MAP kinase pathways in the yeast *Saccharomyces cerevisiae*. Microbiol Mol Biol Rev 1998;62:1264-300.
18. Xu JR. Map kinases in fungal pathogens. Fungal Genet Biol 2000;31:137-52.
19. Wösten HA, Scholtmeijer K. Applications of hydrophobins: current state and perspectives. Appl Microbiol Biotechnol 2015;99:1587-97.
20. Alshahni MM, Shimizu K, Yoshimoto M, Yamada T, Nishiyama Y, Arai T, Makimura K. Genetic and phenotypic analyses of calcineurin A subunit in *Arthroderma vanbreuseghemii*. Med Mycol 2016;54:207-18.
21. Han JH, Lee HM, Shin JH, Lee YH, Kim KS. Role of the MoYAK1 protein kinase gene in *Magnaporthe oryzae* development and pathogenicity. Environ Microbiol 2015;17: 4672-89.
22. Soanes DM, Kershaw MJ, Cooley RN, Talbot NJ. Regulation of the MPG1 hydrophobin gene in the rice blast fungus *Magnaporthe grisea*. Mol Plant Microbe Interact 2002;15: 1253-67.
23. Sammer D, Krause K, Gube M, Wagner K, Kothe E. Hydrophobins in the life cycle of the ectomycorrhizal basidiomycete *Tricholoma vaccinum*. PLoS One 2016;11: e0167773.
24. Yue X, Que Y, Deng S, Xu L, Oses-Ruiz M, Talbot NJ, Peng Y, Wang Z. The cyclin dependent kinase subunit Cks1 is required for infection-associated development of the rice blast fungus *Magnaporthe oryzae*. Environ Microbiol 2017;19:3959-81.
25. Wang Y, Tian L, Xiong D, Klosterman SJ, Xiao S, Tian C. The mitogen-activated protein kinase gene, *VdHog1*, regulates osmotic stress response, microsclerotia formation and virulence in *Verticillium dahliae*. Fungal Genet Biol 2016;88:13-23.
26. Kim DH, Rigling D, Zhang L, Van Alfen NK. A new extracellular laccase of *Cryphonectria parasitica* is revealed by deletion of *Lac*1. Mol Plant Microbe Interact 1995;8:259-66.
27. Powell WA, Van Alfen NK. Differential accumulation of poly(A)+ RNA between virulent and double-stranded RNA-induced hypovirulent strains of *Cryphonectria (Endothia) parasitica*. Mol Cell Biol 1987;7:3688-93.
28. Kumar S, Stecher G, Tamura K. MEGA7: Molecular Evolutionary Genetics Analysis version 7.0 for bigger datasets. Mol Biol Evol 2016;33:1870-4.
29. Henikoff S, Henikoff JG. Amino acid substitution matrices from protein blocks. Proc Natl Acad Sci U S A 1992;89: 10915-9.
30. Jones DT, Taylor WR, Thornton JM. The rapid generation of mutation data matrices from protein sequences. Comput Appl Biosci 1992;8:275-82.
31. Saitou N, Nei M. The neighbor-joining method: a new method for reconstructing phylogenetic trees. Mol Biol Evol 1987;4:406-25.
32. Bailey TL, Johnson J, Grant CE, Noble WS. The MEME Suite. Nucleic Acids Res 2015;43:W39-49.
33. Bailey TL, Boden M, Buske FA, Frith M, Grant CE, Clementi L, Ren J, Li WW, Noble WS. MEME SUITE: tools for motif discovery and searching. Nucleic Acids Res 2009;37:W202-8.
34. de Nadal E, Casadomé L, Posas F. Targeting the MEF2-like transcription factor Smp1 by the stress-activated Hog1 mitogen-activated protein kinase. Mol Cell Biol 2003;23:229-37.
35. Su JC, Lin KL, Chien CM, Tseng CH, Chen YL, Chang LS, Lin SR. Furano-1,2-naphthoquinone inhibits EGFR signaling associated with G2/M cell cycle arrest and apoptosis in A549 cells. Cell Biochem Funct 2010;28:695-705.
36. Shore P, Sharrocks AD. The ETS-domain transcription factors Elk-1 and SAP-1 exhibit differential DNA binding specificities. Nucleic Acids Res 1995;23:4698-706.
37. Qu X, Yu B, Liu J, Zhang X, Li G, Zhang D, Li L, Wang X, Wang L, Chen J, et al. MADS-box transcription factor SsMADS is involved in regulating growth and virulence in *Sclerotinia sclerotiorum*. Int J Mol Sci 2014;15:8049-62.